Available online at www.sciencedirect.com
ScienceDirect
International Journal of Mass Spectrometry 261 (2007) 1–12
International Journal of Mass Spectrometry
www.elsevier.com/locate/ijms

An investigation of the mobility separation of some peptide and protein ions using a new hybrid quadrupole/travelling wave IMS/oa-ToF instrument

Steven D. Pringle [a], Kevin Giles [a,**], Jason L. Wildgoose [a], Jonathan P. Williams [b,*], Susan E. Slade [b], Konstantinos Thalassinos [b], Robert H. Bateman [a], Michael T. Bowers [c], James H. Scrivens [b]

[a] *Waters MS Technologies Centre, Micromass UK Ltd., Floats Rd., Wythenshawe, Manchester M23 9LZ, UK*
[b] *Department of Biological Sciences, University of Warwick, Gibbet Hill Rd., Coventry CV4 7AL, UK*
[c] *Department of Chemistry, University of California at Santa Barbara, Santa Barbara, CA, USA*

Received 24 February 2006; received in revised form 20 July 2006; accepted 20 July 2006
Available online 6 September 2006

Abstract

Ion mobility coupled with mass spectrometry has evolved into a powerful analytical technique for investigating the gas-phase structures of bio-molecules. Here we present the mobility separation of some peptide and protein ions using a new hybrid quadrupole/travelling wave ion mobility separator/orthogonal acceleration time-of-flight instrument. Comparison of the mobility data obtained from the relatively new travelling wave separation device with data obtained using various other mobility separators demonstrate that whilst the mobility characteristics are similar, the new hybrid instrument geometry provides mobility separation without compromising the base sensitivity of the mass spectrometer. This capability facilitates mobility studies of samples at analytically significant levels.

Keywords: Ion mobility; Travelling wave; Mass spectrometry; Conformation

1. Introduction

A wide variety of diseases previously thought to be unrelated, such as prion diseases, diabetes and cancer, share the pathological feature of aggregated misfolded protein deposits [1]. This suggests the exciting possibility that these 'protein-misfolding diseases' are linked by common principles. Ion mobility (IM) spectrometry in combination with mass spectrometry (MS) provides a specific probe for investigating the structural and conformational properties of bio-molecules in the gas phase [2–7] and therefore has the potential to be of great value to this research. Sensitivity is a key requirement for these measurements since biologically relevant concentrations need to be examined.

IM spectrometry relies on separation of a packet of ions based on mobility differences as they drift through an inert gas under the influence of a weak electric field. Classical ion mobility devices, or drift tubes, use a uniform, static, electric field to drive ions through the background gas. The physical principles behind drift tube devices are well understood [8,9] and mobility values obtained can be used to derive gas-phase collision cross-sections (Ω) for comparison with theory [4,5,10,11] using the derived expression:

$$\Omega = \frac{3ze}{16N}\left[\frac{2\pi}{\mu k_b T}\right]^{0.5}\frac{1}{K_0} \quad (1)$$

where N is the background gas number density, ze the ionic charge, μ the reduced mass of the ion–neutral pair, k_b is Boltzmann's Constant, T the gas temperature and K_0 is the reduced mobility (=measured mobility corrected to 273.2 K and 760 Torr).

The last decade has seen extensive development in IM–MS techniques. Perhaps the more important advances from an ana-

* Corresponding author. Tel.: +44 2476522157.
** Corresponding author.
E-mail addresses: Kevin_Giles@waters.com (K. Giles), j.p.williams@warwick.ac.uk (J.P. Williams).

1387-3806/$ – see front matter © 2006 Elsevier B.V. All rights reserved.
doi:10.1016/j.ijms.2006.07.021

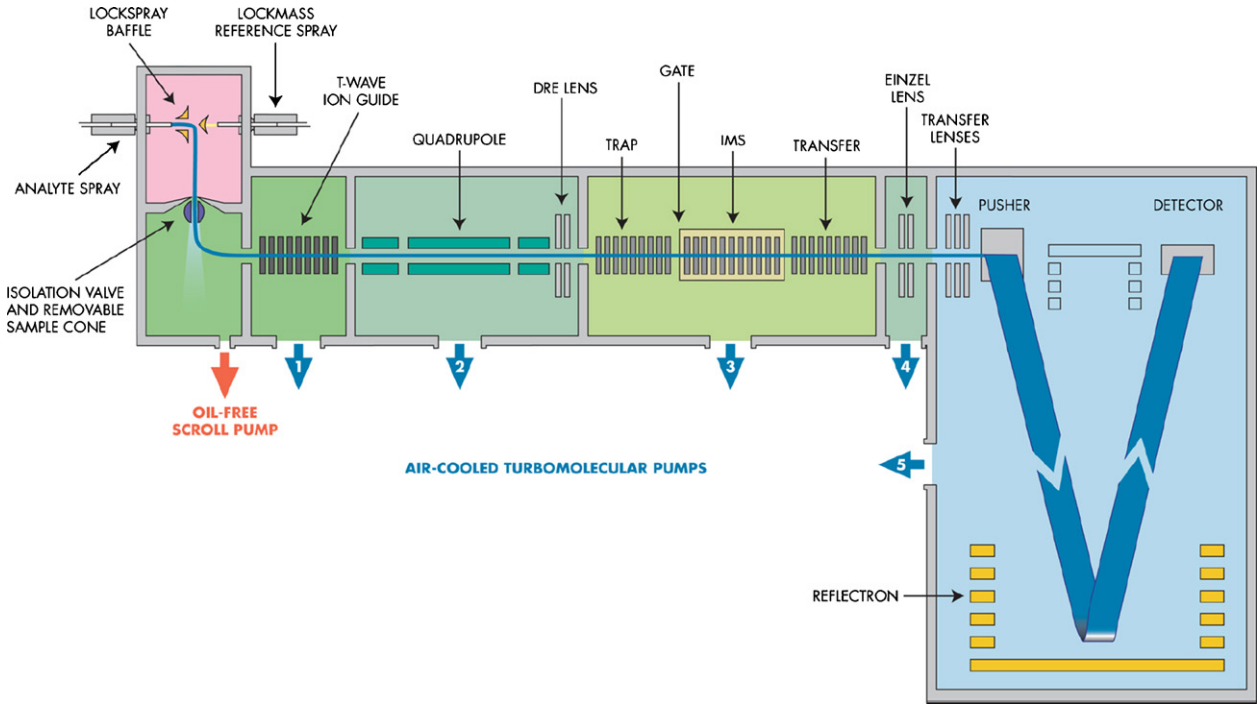

Fig. 1. A schematic diagram of the Synapt HDMS system. All of the turbomolecular pumps have 220 l/s pumping speed (model EXT255H, Edwards, Crawley, UK) and are backed by a 35 m^3/h scroll pump (model XDS35i, Edwards, Crawley, UK).

lytical standpoint have been those which help to address inherent sensitivity issues associated with classical drift tubes and provide faster mass spectral acquisition. Typically, drift tube devices suffer from poor sensitivity due to the low duty cycle related to gating packets of ions into the device and due to ion radial diffusion beyond the diameter of sampling apertures in the mass spectrometer. In a previous study, the low duty cycle was effectively overcome in sub-ambient pressure drift cells through use of a Paul geometry ion trap to both accumulate ions whilst the previous mobility separation was occurring, and then to inject them into the drift tube [12]. Other ion storage geometries have since been used to improve duty cycle [13,14]. Alternatively the issue of duty cycle can be somewhat circumvented through use of discontinuous ion sources such as MALDI, where the ion plume from each laser shot can provide the packet for mobility separation [4,6,15–17]. The effect of ion loss due to radial diffusion has been lowered through use of a periodic focussing dc drift tube design [6,16,17], or has been essentially eliminated through use of radio frequency (RF) ion guides with axial fields as the mobility separator [18–20]. A high-field focussing element at the exit of the mobility cell has also been shown to improve ion transmission [21]. More recently, the combined use of ion funnels before and after the drift tube has been shown to provide essentially lossless transmission [22,23]. The first funnel accumulates ions and pulses them into the drift tube and the second is used to re-axialize the radially diffuse mobility-separated ions. In terms of mass spectral acquisition, the use of ToF [24] and in particular orthogonal acceleration (oa) ToF technology provides an analyser which is capable of providing full mass spectra on timescales short enough to enable profiling of millisecond wide ion mobility peaks; a capability not possible with mass analysers such as quadrupoles or ion traps.

A different approach to mobility separating ions using a travelling voltage wave incorporated in a RF ion guide has recently been reported [25,26]. This technique shows high transmission efficiency and a separative power comparable with conventional drift cell approaches albeit at only moderate resolution. Here we present data on the mobility separation and mass analysis of a number of peptides and proteins obtained using a new hybrid quadrupole/IM separator/oa-ToF instrument where the IM separator is based on the travelling wave device reported previously. The results obtained are compared with previously reported data obtained using other mobility separators.

2. Instrumentation

A schematic diagram of the hybrid quadrupole/IM separator/oa-ToF instrument (the Synapt HDMS system-Waters Corp., Milford, USA) is shown in Fig. 1. The IM section comprises three travelling wave-enabled stacked ring ion guides (SRIGs) as shown in more detail in Fig. 2. The trap ion guide is used to accumulate ions during the previous mobility separation then release an ion packet into the IM ion guide for mobility separation. The transfer ion guide is used to convey the mobility-separated ions to the oa-ToF for mass analysis.

2.1. Travelling wave stacked ring ion guides

A full description of the mode of operation of stacked ring ion guides with travelling waves is given elsewhere [25] and so will only be described briefly here. The ion guide comprises a series of planar electrodes arranged orthogonally to the ion

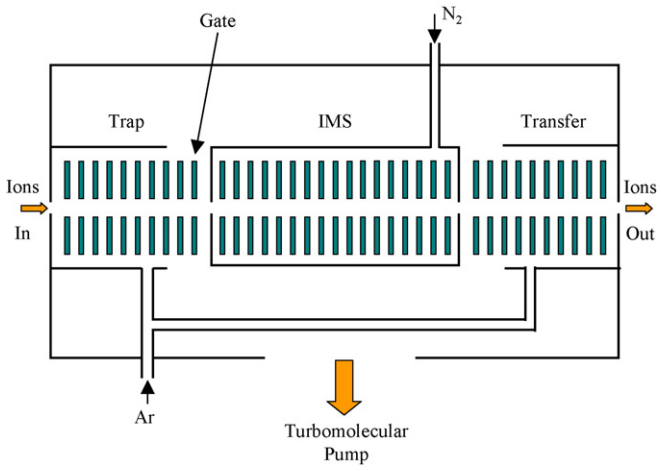

Fig. 2. A schematic diagram of the IMS section of the Synapt, comprising three travelling wave ion guides labelled, trap, IMS and transfer.

transmission axis, as shown in Fig. 3. Opposite phases of an RF voltage are applied to adjacent electrodes and provide a radially confining effective potential barrier [27]. In the presence of a background gas, ion axial motion through a SRIG can be significantly slowed or stopped due to the presence of axial traps generated by the ring geometry. To propel ions through the gas, a transient dc voltage is superimposed on the RF applied to a pair of adjacent electrodes in a repeating sequence along the length of the device. The series of potential hills so generated are subsequently applied to the next pair of electrodes downstream at regular time intervals providing a continuous sequence of 'travelling waves'. The ions within the device are driven away from the potential hills and consequently are carried through the device with the waves, minimising their transit time (see Fig. 4). All the travelling wave ion guides (TWIGs) used in the IM section of the instrument have 5 mm diameter ion transmission apertures, 0.5 mm electrode thickness and a centre-to-centre spacing of 1.5 mm. The RF voltage used is

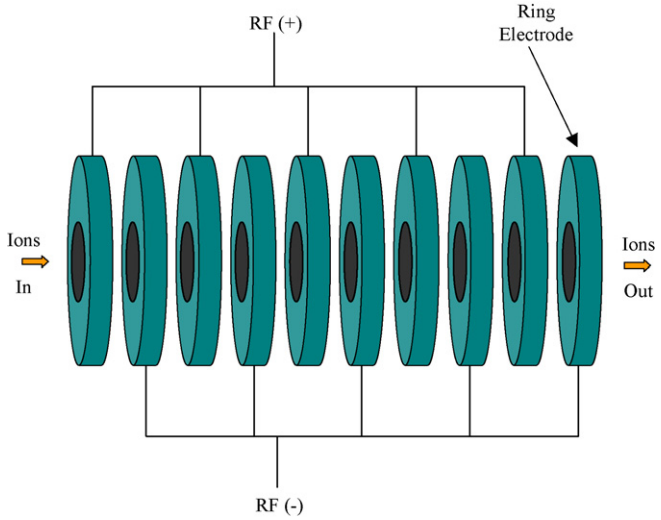

Fig. 3. A stacked ring ion guide (SRIG).

at a frequency of 2.7 MHz and is of variable amplitude up to 400 V pk–pk.

2.1.1. Travelling wave IMS (TWIMS)

The TWIMS consists of 61 electrode pairs with a pulse repeat pattern of six pairs and is 185 mm long. The cell is gas tight except for 2 mm diameter ion entrance and exit apertures and can be operated at pressures up to 1 mbar, the gas is supplied by a 0–200 ml/min mass flow controller (Bronkhorst, Sawston, UK). Travelling waves of up to 25 V are used with velocities in the range of 300–600 m/s.

2.1.2. Trap and transfer TWIG

The trap and transfer TWIGs consist of 33 electrode pairs with RF applied and are 100 mm long. The final electrode on the trap TWIG is dc-only and its voltage is modulated (typically ±5 V with respect to the ion guide dc offset) to periodically gate ions into the IMS. Both cells are enclosed but are not completely gas tight; they share a common gas supply from a 0 to 10 ml/min mass flow controller (Bronkhorst, Sawson, UK). Typically these cells are operated at pressures in the low 10^{-2} mbar range. Generally no travelling wave is used in the trap TWIG, whereas the transfer TWIG has a continually running 1–2 V, 300 m/s wave to ensure the mobility separation is maintained on transit to the oa-ToF.

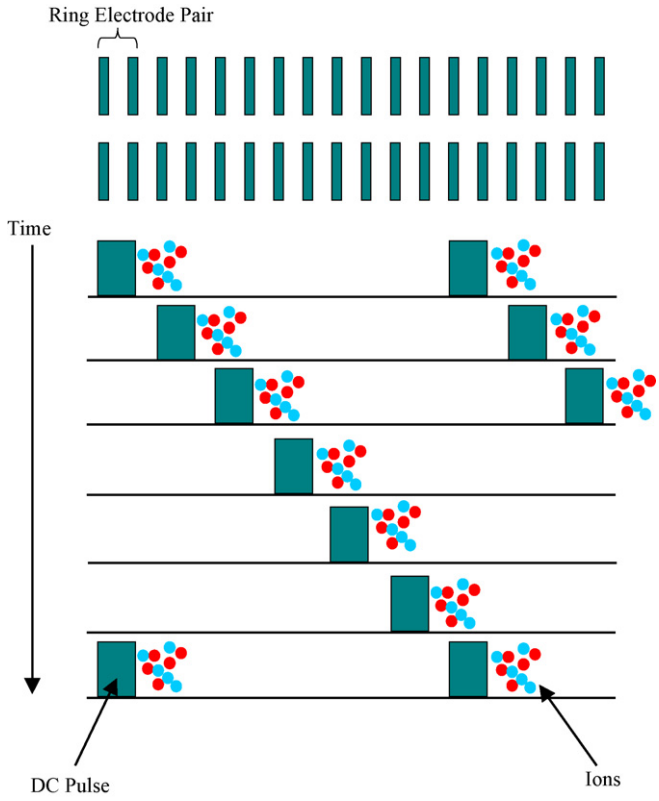

Fig. 4. Illustration of the operation of a TWIG for ion propulsion in the presence of background gas.

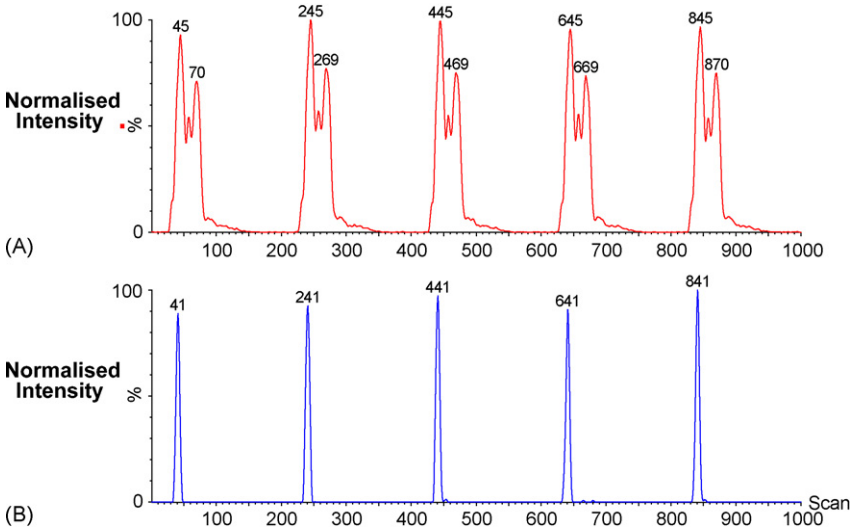

Fig. 5. Illustration of the mode of mobility acquisition on the Synapt instrument: (A) shows the ATDs of the four peptide mix, the five sequential acquisitions are 5 s summations; (B) shows the ATD for the doubly charged ion of bradykinin (TWIMS: 7 V pulse).

2.2. Travelling wave ion mobility separation

The means of efficiently transporting ions through a SRIG using a travelling voltage wave was outlined above, however, it has been shown previously that use of elevated pressures in a TWIG can result in ion species being unable to keep up with the wave front as a result of increased drag [25]. As a consequence, ion species periodically slip behind the waves but, on average, are propelled in the direction that the wave is travelling. Ion species of high mobility slip behind the waves less often than species of low mobility and so are transported through the device more quickly, thus mobility-based separation of ions occurs.

2.3. Ion mobility data acquisition

Recording the temporal arrival profile of ions is achieved by synchronisation of the oa-ToF acquisition with the gated release of ions from the trap TWIG into the TWIMS. Following the gate pulse, the subsequent 200 orthogonal acceleration pushes (mass spectra) of the ToF analyser are recorded, giving an overall mobility recording time of $200 \times t_{pp}$, where t_{pp} is the pusher period. Following the next gated release of ions, a further 200 mass spectra are acquired and added to the corresponding spectra from the previous acquisition. This process is repeated for a predefined period and subsequently the 200 spectra are saved and the next summation period begins.

2.4. Modes of operation

The geometry of the Synapt HDMS instrument, shown in Figs. 1 and 2, enables various types of IM analyses to be undertaken. Since the trap and transfer TWIGs operate at approximately standard collision cell pressures it is possible to fragment ions in either or both of these regions enabling mobility separation of product ions, fragmentation of mobility-separated precursor ions and fragmentation of mobility-separated product ions. The latter example is essentially an MS^3 type experiment with the advantage that all first and second generation product ions are recorded at the same time. Alternatively, through use of lower collision energies in these regions, the mobility separation of precursor ion species can be obtained. These types of analyses

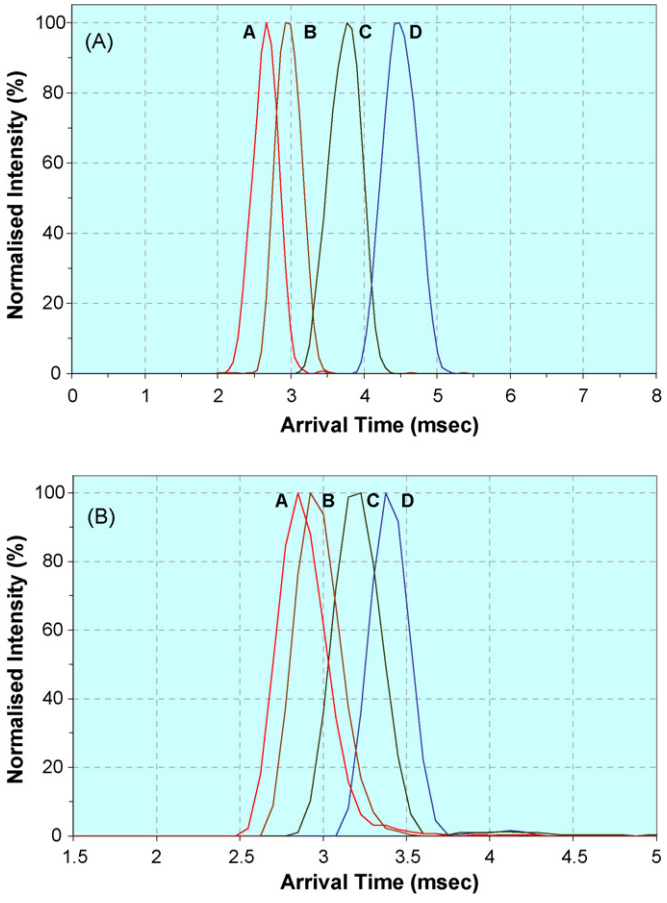

Fig. 6. (A) ATDs of the doubly charged ions of the four peptide mix separated in the TWIMS. A, bradykinin; B, LHRH; C, substance P; D, bombesin (TWIMS: 7 V pulse). (B) ATDs of the doubly charged ions of the four-peptide mix separated in the SRIG with axial field [19].

can be performed on essentially all ion species generated form the source by operating the quadrupole in RF-only mode, or can be performed on mass-selected species with the quadrupole in resolving mode. Some of these modes of operation are presented below to illustrate the capability of the instrument.

2.5. Operating conditions

The instrument was operated in positive ion electrospray mode and samples were infused using the built-in syringe drive. The quadrupole was generally operated in RF-only mode for full

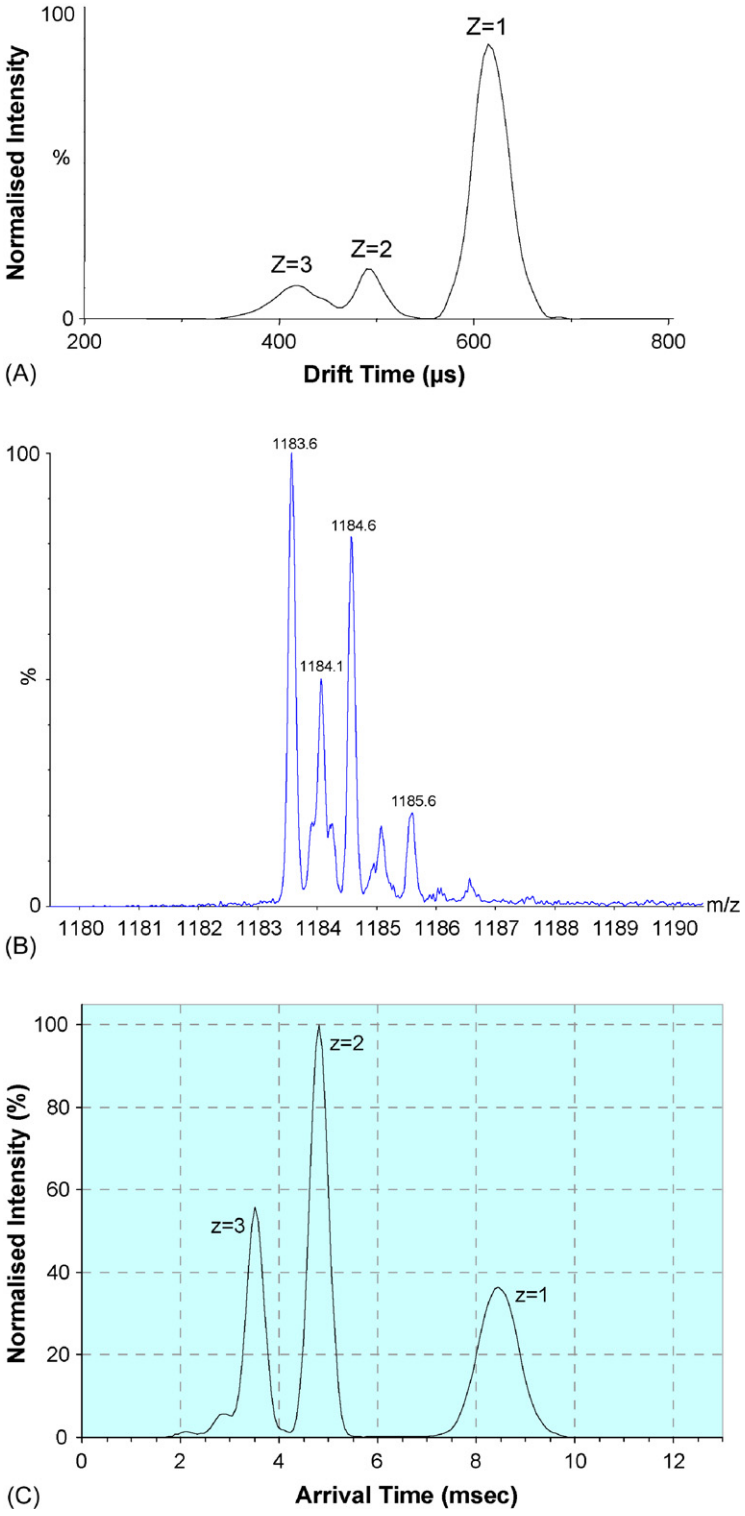

Fig. 7. (A) ATD of the LHRH ions at *m/z* 1183 obtained using a dc drift tube (Bowers, unpublished data), where *z* denotes the oligomeric form: $(_zM + _zH)^{z+}$. (B) Mass spectrum of LHRH obtained using the Synapt with no mobility separation. (C) ATD of the LHRH ions at *m/z* 1183 separated using the TWIMS. (D) Mass spectra obtained from the labelled peaks in (C) (TWIMS: 8 V pulse).

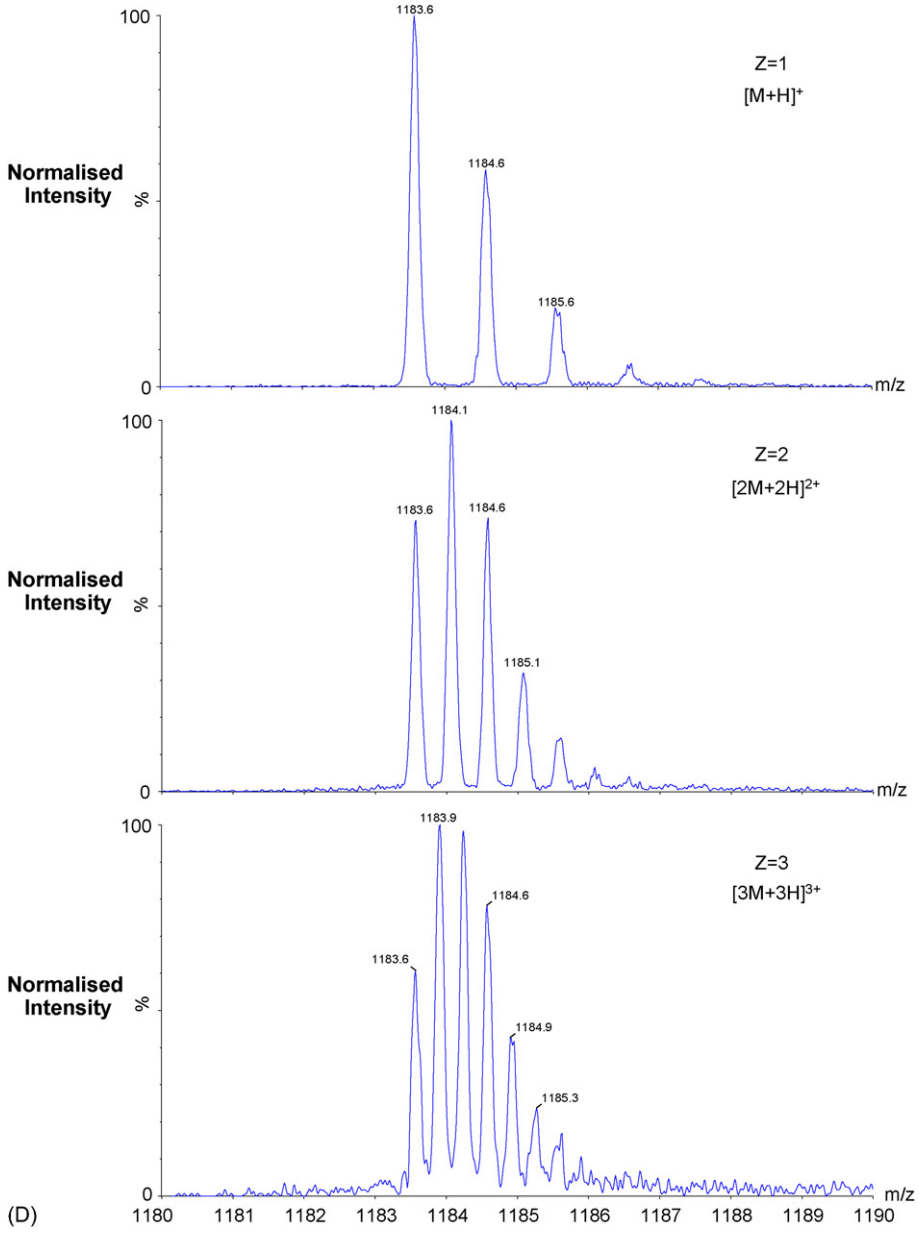

Fig. 7. (*Continued*).

mobility spectra recording and the oa-ToF nominally at 10,000 resolution FWHM. The instrument control and data acquisition software was based on MassLynx v4.1. Pressures were measured in the trap, IMS and transfer TWIGs using active pirani gauges (model APG-L, Edwards, Crawley, UK) calibrated against nitrogen.

In these studies an IMS pressure of 0.5 mbar N_2 and a trap/transfer pressure of 2×10^{-2} mbar Ar were used unless stated otherwise. The RF amplitude used on the trap, IMS and transfer TWIGs was 300 V pk–pk and dc offsets were +20, +3 and 0 V, respectively, with respect to ground. IMS travelling wave velocities of 300 m/s were used unless stated otherwise, the wave pulse heights are reported for each set of experiments presented.

2.6. Sample preparation

Peptides used in the investigation were bradykinin, luteinizing hormone-releasing hormone (LHRH), substance P and bombesin and these were analysed at a concentration of 200 fmol/μL in water:acetonitrile + 0.1% formic acid. The isomeric peptides Ser-Asp-Gly-Arg-Gly and Gly-Arg-Gly-Asp-Ser were analysed at a concentration of 400 fmol/μL in water:acetonitrile + 0.1% formic acid. LHRH was investigated for aggregate formation at a concentration of 8 pmol/μL in 50:50 water:acetonitrile. Glu-Fibrinopeptide B was analysed at 100 fmol/μL in water:methanol + 0.1% formic acid. Proteins used in the investigation were cytochrome *c* (equine), myoglobin, lysozyme and α-lactalbumin and were analysed at a

concentration of 1 pmol/μL in water:acetonitrile + 0.1% formic acid. A standard mixture of the tryptic digests of yeast alcohol dehydrogenase, rabbit glycogen phosphorylase b, bovine serum albumin and yeast enolase was analysed sub-pmol/μL level in water:acetonitrile + 0.1% formic acid. All samples, with the exception of the digest (Waters MassPrep Digestion Standard Mix 2, Waters, Milford, USA), were purchased from Sigma–Aldrich Company Limited (Poole, U.K.) and used without further purification. All were introduced to the electrospray source by direct infusion at a flow rate of 5 μL/min.

3. Results and discussion

3.1. Arrival time distributions

The recorded arrival time of an ion species at the detector following release at the gate is commonly referred to as the arrival time distribution (ATD). Fig. 5(A) shows the ion mobility separation of bradykinin, LHRH, substance P and bombesin for five sequential acquisitions (each of 5 s). Each mobility acquisition is 200 'scans' long and with a pusher period of 65 μs this equates to 13 ms. Fig. 5(B) is the extracted ATD of the doubly charged bradykinin ion. From Fig. 5(B) an arrival time of 2.67 ms can be calculated for this ion (scan number (41) × pusher period (0.065 ms)). In all subsequent figures the *x*-axis has been converted from scan number to milliseconds for clarity. No corrections have been made in the displayed ATDs for the time taken for ions to be transferred from the exit of the IM cell to the ToF analyser ($t < 0.5$ ms).

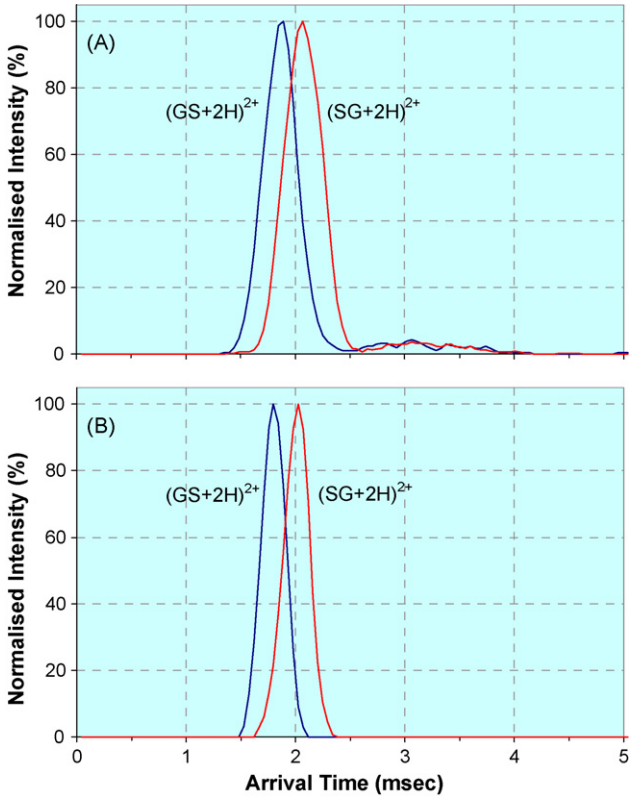

Fig. 8. ATDs of the doubly charged ions of the isomeric species Ser-Asp-Gly-Arg-Gly (SG) and Gly-Arg-Gly-Asp-Ser (GS) separated in the TWIMS with a 300 m/s wave and:(A) 0.5 mbar N_2, 5.5 V pulse (B) 1.0 mbar N_2, 11 V pulse.

3.2. Separation of peptides using ion mobility

3.2.1. Peptide mixture

The extracted ATDs of the doubly charged precursor ions from the mixture of bradykinin, LHRH, substance P and bombesin separated in the TWIMS are shown in Fig. 6(A). For comparison, the separation obtained previously using a SRIG with an axial dc field (13.2 V/cm over the 15.2 cm drift region) in nitrogen gas at a pressure of around 2.5 mbar is shown in Fig. 6(B) [19]. Whilst the character of the separation is the same in both devices (correlating with previously determined collision cross-sections for these ion species [19,28]), the degree of separation is greater in the TWIMS case, even though the cell pressure is ∼5 times lower than in the SRIG experiments. A further interesting point is that whilst the arrival time data from the SRIG system could be used to determine average collision cross-sections for these species that were in good agreement with the previous measurements [19], the TWIMS data indicate a different arrival time and mobility relationship than the inverse dependence observed in dc systems. An investigation into this difference will be presented in a separate publication.

3.2.2. LHRH aggregation

The study of peptide aggregation processes forms an important part of research into diseases such as Alzheimer's, Parkinson's and Huntington's which are linked with misfolded protein structures. The observation of peptide aggregates/oligomers by ESI-MS is not uncommon and has been studied previously using dc drift tube systems [14,29,30]. The potential of the TWIMS for separation of such species has been demonstrated using bradykinin [25] and is investigated further here.

Previous investigations of the singly charged protonated LHRH at *m/z* 1183 using a dc drift tube [14] revealed multiple features in the ATD which were believed to be due to the presence of oligomers of the form $(zM + zH)^{z+}$ (see Fig. 7(A)).

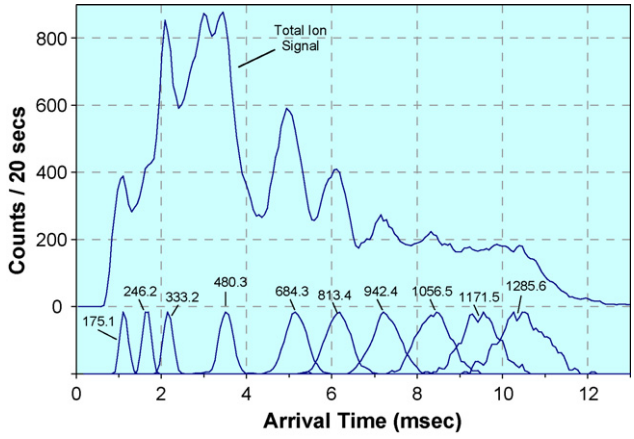

Fig. 9. ATD of the fragment ions of the doubly charged precursor ion of Glu-Fibrinopeptide B, showing the ATD of both the sum of the ion species (for a 20 s acquisition) and the mass-selected normalised ATDs (*m/z* labelled) for the more intense fragments (TWIMS: 600 m/s, 12 V pulse).

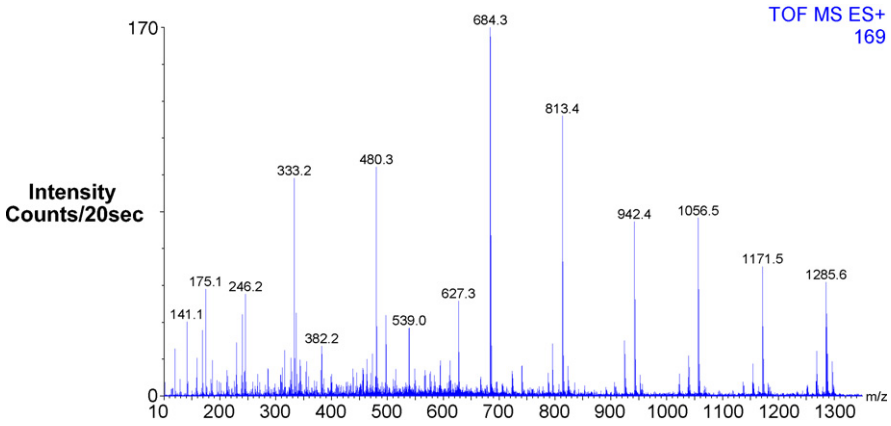

Fig. 10. Mass spectrum of the fragment ions of the doubly charged precursor ion of Glu-Fibrinopeptide B obtained by summing the all data from the ATD shown in Fig. 9.

The mass spectrum obtained in the present study for LHRH at around *m/z* 1183 without mobility separation is shown in Fig. 7(B). It is apparent from this figure that more than just singly charged species are present however it is not easy to say with any confidence what the other components are. The ATD of the ions around *m/z* 1183 obtained using the TWIMS is shown in Fig. 7(C), the similarity with the drift tube data in 7(A) is immediately apparent. The three main peaks have been labelled $z = 1$–3 corresponding to ion arrival times of 8.5, 4.8 and 3.5 ms, respectively. The present instrument offers significant experimental advantage over the previously used quadrupole-based drift tube system in that, due to the use of the oa-ToF analyser, full mass spectra can be obtained for each peak in the ATD. Fig. 7(D) shows the mass spectra obtained from the three labelled peaks in Fig. 7(C). The mass spectra clearly show the presence of the singly charged monomer ($z = 1$) together with the doubly charged dimer ($z = 2$) and triply charged trimer ($z = 3$). On closer inspection of the ATD in Fig. 7(C), the presence of peaks at shorter times than for the $z = 3$ species suggests that still higher order multimers may be present, however, the weak signals precluded unambiguous confirmation in the mass spectra.

3.2.3. Mobility study of isomeric peptides

A particular useful feature of IMS is the capability to separate isomeric species if they differ sufficiently in collision cross-section. In order to establish the separation capability of the TWIMS device a study of two isomeric peptides with sequence Ser-Asp-Gly-Arg-Gly (SG) and Gly-Arg-Gly-Asp-Ser (GS) has been carried out. A previous mobility study reported baseline separation in the ATDs of the doubly charged precursor ions on a high-resolution dc drift tube at atmospheric pressure [31]. From these data a 5% difference in collision cross-section between the two doubly charged isomeric ions was determined.

In the present study, each peptide was infused into the instrument separately and the ATD recorded following separation in the TWIMS. Fig. 8(A) shows the ATDs of the doubly charged precursor ion at *m/z* 246 where the TWIMS was operated at 0.5 mbar N_2 with a 5.5 V/300 m/s wave. From the ATDs the drift time has been calculated to be 1.89 ms for $[GS + 2H]^{2+}$ and 2.07 ms for the less mobile ion $[SG + 2H]^{2+}$. These data are in accord with the previous study where the $[GS + 2H]^{2+}$ ion was calculated to have a smaller cross-section than $[SG + 2H]^{2+}$, although the resolution afforded by the TWIMS device is lower than that of the high-resolution dc drift tube. To try and improve the resolution of the TWIMS the gas pressure was raised to 1.0 mbar and the wave pulse height increased to 11 V. The resultant ATDs for the two peptides are shown in Fig. 8(B) where it can be seen that the increase in pressure has increased the resolution by approximately 50%. Overall, whilst the resolution of the TWIMS is not high, it does provide the potential to distinguish between these isomeric peptides that differ in collision cross-section by only 5%.

3.2.4. Mobility separation of peptide fragments

As stated earlier, the geometry of the Synapt HDMS instrument (see Figs. 1 and 2) enables ion species to be fragmented on entry to the trap TWIG, such that the fragment ions are accumulated prior to their mobility separation. For this study 100 fmol/μL of Glu-Fibrinopeptide B (in 50:50 methanol:water 1% formic acid) was infused into the electrospray source at 5 μL/min and the $(M + 2H)^{2+}$ ion at *m/z* 785.6 selectively transmitted through the quadrupole and fragmented in the Trap TWIG through use of 30 V injection voltage. Fig. 9 shows both the ATDs of the sum of all the fragment ions over a

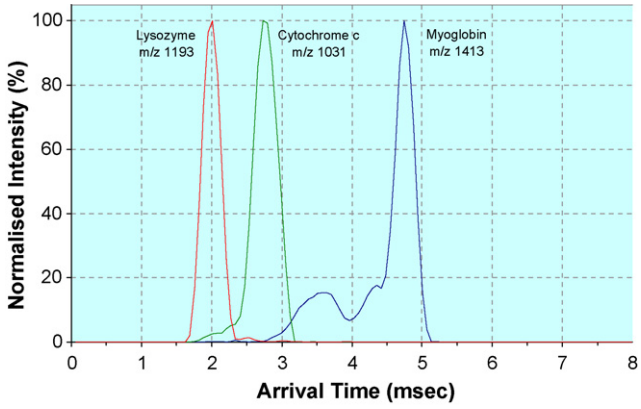

Fig. 11. ATDs of the +12 charge states of lysozyme, cytochrome *c* and myoglobin obtained using the TWIMS (TWIMS: 7 V pulse).

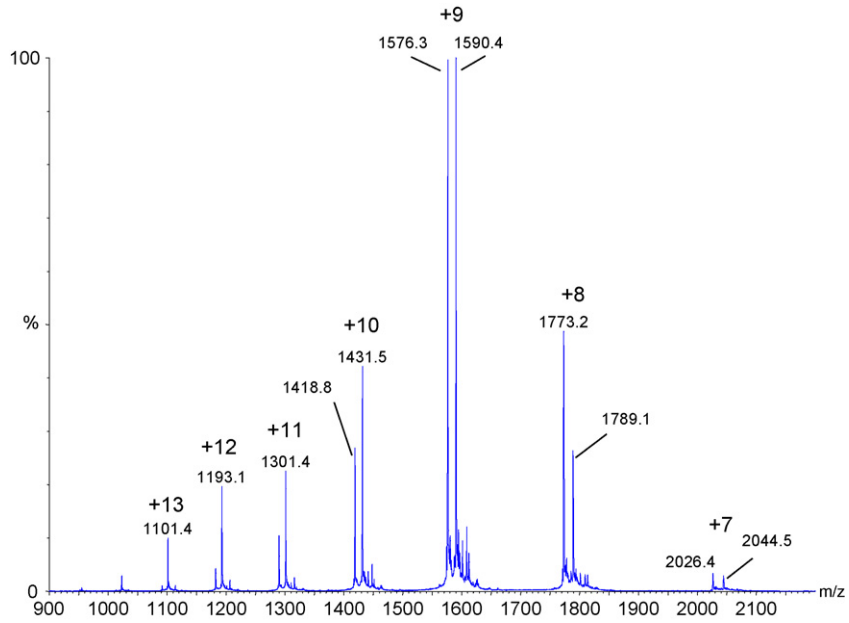

Fig. 12. Mass spectrum of a mixture of α-lactalbumin (14,186 Da) and lysozyme (14,313 Da) illustrating the charge state distribution.

100–1500 *m/z* range and selected ATDs for the most intense *m/z* species for a 20 s acquisition period. The associated mass spectrum produced by combining all the mobility data in the 20 s acquisition is shown in Fig. 10. These data illustrate that it is possible to obtain mobility separations using this instrument with sample concentrations equivalent to those used in standard MS applications. This is as a result of the combination of ion accumulation prior to mobility separation and radial ion confinement in the TWIMS device and provides a significant increase in transmission over standard dc drift tubes.

3.3. Protein conformational studies

There is now considerable evidence that for many systems the gas-phase conformation of ions studied by mass spectrometry are closely related to the solution-phase structure. Pioneering work by Last and Robinson [32] demonstrated "compelling evidence for preservation of tertiary structure under controlled conditions" using H/D exchange and, more recently, IM–MS results obtained by Ruotolo et al. [26] indicate that multi-protein complexes retain their liquid phase structure in the gas phase. A review by Heck and Van Den Heuvel [33] describing the analysis of intact protein complexes by mass spectrometry strongly supports this view. Perhaps the most compelling evidence is the work by Cooks and co-workers [34,35] where ESI generated trypsin and lysozyme proteins ions were sampled into the mass spectrometer and, using 'soft-landing' experiments, it was subsequently demonstrated that the proteins had retained their biological activity.

3.3.1. Lysozyme, cytochrome c and myoglobin mobility separation

Fig. 11 shows the ATDs for the +12 charge state of lysozyme (14,313 Da), cytochrome *c* (equine) (12,361 Da) and myoglobin (16,951 Da) from the infusion of a 1 pmol/μL mixture. Previous cross-section measurements [28,36] of the +12 charge state for these proteins have indicated myoglobin to be the largest and lysozyme the smallest. The TWIMS data are in accord with these measurements. Good separation is achieved for the +12 charge states of these proteins; the lysozyme and cytochrome *c* ATDs show little evidence for additional conformers, however, the myoglobin ATD shows the presence of a number of additional conformers at shorter arrival times than the main peak.

3.3.2. Lysozyme and α-lactalbumin mobility separation

The two proteins, α-lactalbumin (14,186 Da) and lysozyme (14,313 Da) have a mass difference of approximately 1% and have been studied previously using IM–MS [19]. The mass spectrum of a mixture of these proteins is given in Fig. 12 and shows the formation of charge states from +7 to about +15 from the presence of peaks over the *m/z* range 900–2044.

The ATDs for the same charge state ions of each protein are similar, suggesting similar collision cross-sections, as can be seen for the +9 and +12 species in Fig. 13(A). The +8 charge state for each protein exists in two conformations as evidenced by the double peaks in Fig. 13(B), and again the ATDs are similar between the two proteins. The lower mobility peaks at around 3.2 ms follow the increasing arrival time trend of the higher charge states in Fig. 13(A), however, the other conformation has a significantly higher mobility indicating a much reduced collision cross-section. These types of observations have been made on many occasions for protein species and are attributed to the presence of both the more extended, denatured, form of the protein, and the more compact, native, form [4,5,14,28,37–39]. A similar ATD profile is observed for the 7+ charge state of α-lactalbumin, Fig. 13(C), where the conformer having the smaller cross-section predominates (arrival time 2.4 ms), in keeping with

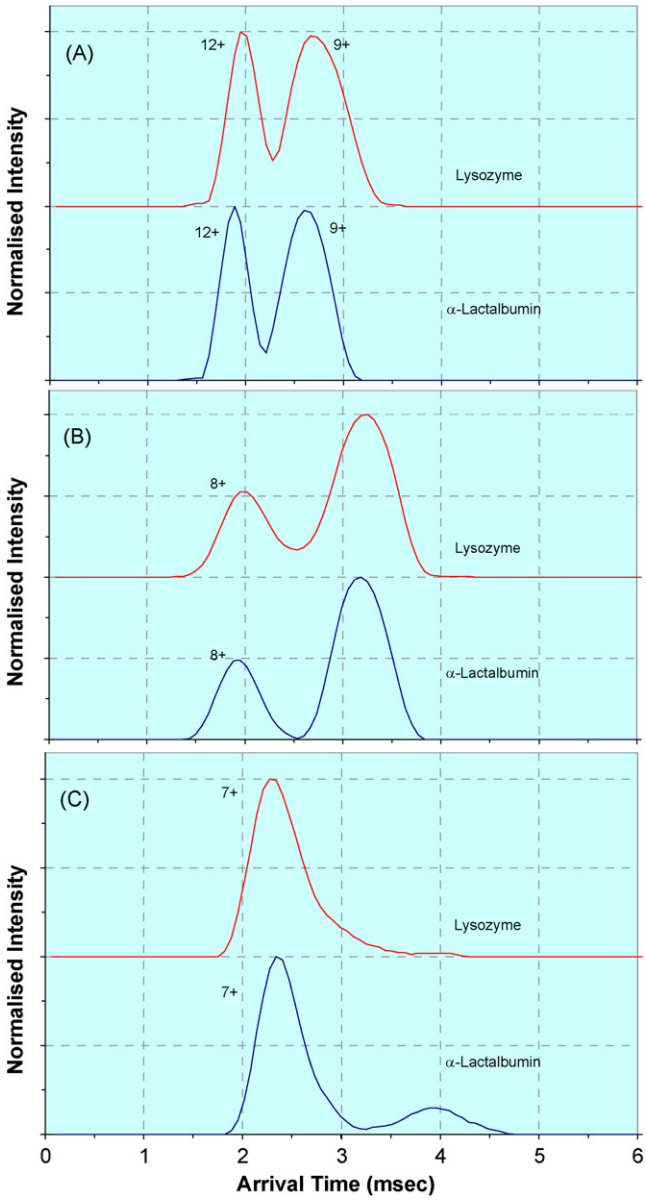

Fig. 13. (A) ATDs of the +9 and +12 charge states of α-lactalbumin and lysozyme; (B) ATDs of the +8 charge state of α-lactalbumin and lysozyme; (C) ATDs of the +7 charge state of α-lactalbumin and lysozyme (TWIMS: 10 V pulse).

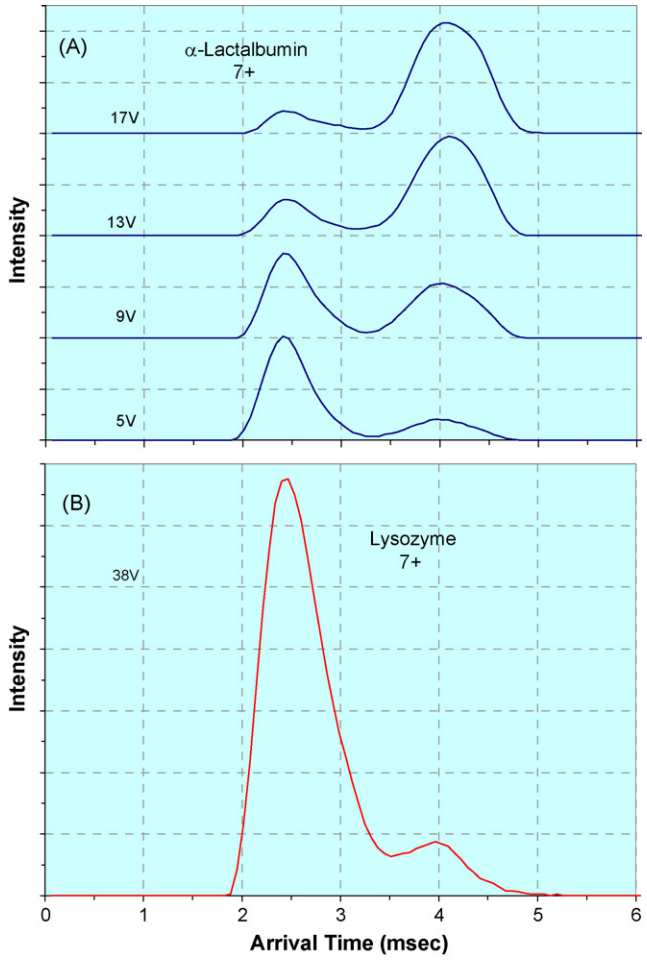

Fig. 14. (A) ATDs illustrating the effect of ion injection energy on the different conformations of the +7 charge state ion of α-lactalbumin (values shown are injection voltages). (B) ATD illustrating the effect of ion injection energy on the different conformations of the +7 charge state ion of lysozyme (TWIMS: 10 V pulse).

previous observations [19]. The ATD for the 7+ charge state of lysozyme, shown in Fig. 13(C), is, by inference from the α-lactalbumin ATD, predominantly the more compact, higher mobility conformation.

The data shown in Fig. 13 were obtained with relatively low ion injection energies into the Argon-filled trap TWIG (approx. 3 V injection). Fig. 14(A) shows the effect on the ATD of increasing the injection energy into the trap TWIG for the 7+ charge state of α-lactalbumin. It is apparent that increasing energy promotes rearrangement of the more compact conformer to the structure of the lower mobility form. Again, this type of behaviour with increasing 'activation' energy has been observed previously for other protein species [4,5]. Interestingly, significantly higher injection energy is required to promote re-

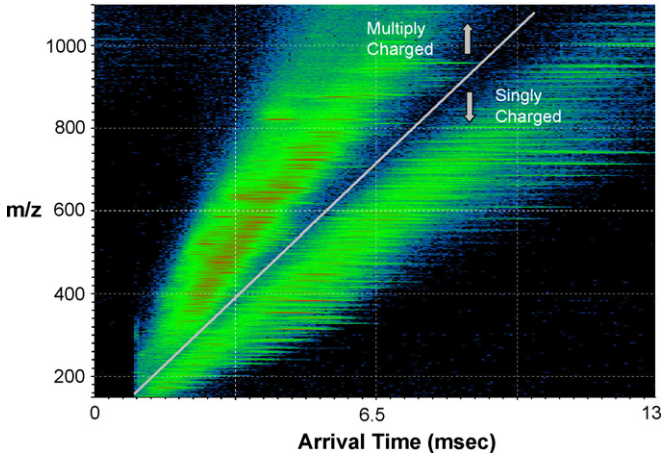

Fig. 15. A 2D plot of ion arrival time vs. *m/z* for a protein digest mixture obtained using the TWIMS (TWIMS: 6 V pulse).

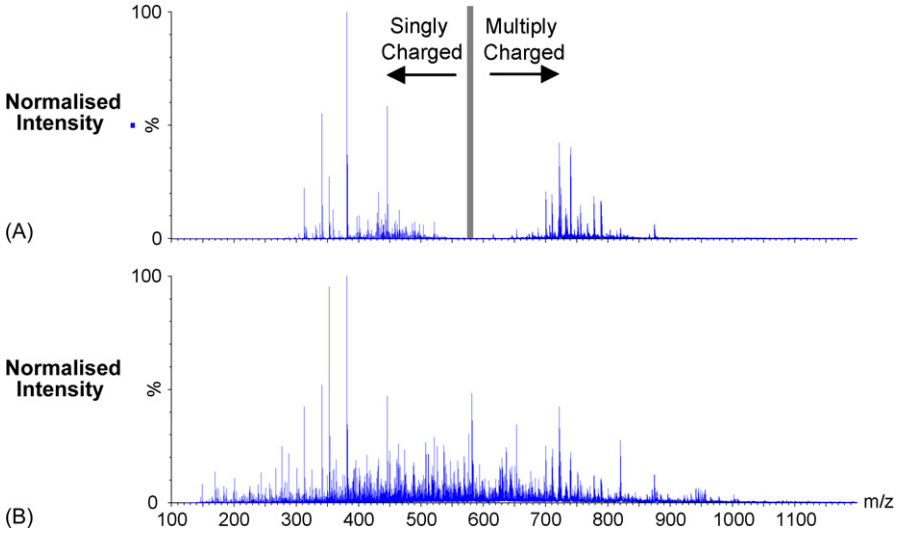

Fig. 16. (A) Mass spectrum obtained by summing the mobility data in Fig. 15 over arrival times from 4.9 to 5.2 ms. (B) The mass spectrum obtained by summing over all arrival times.

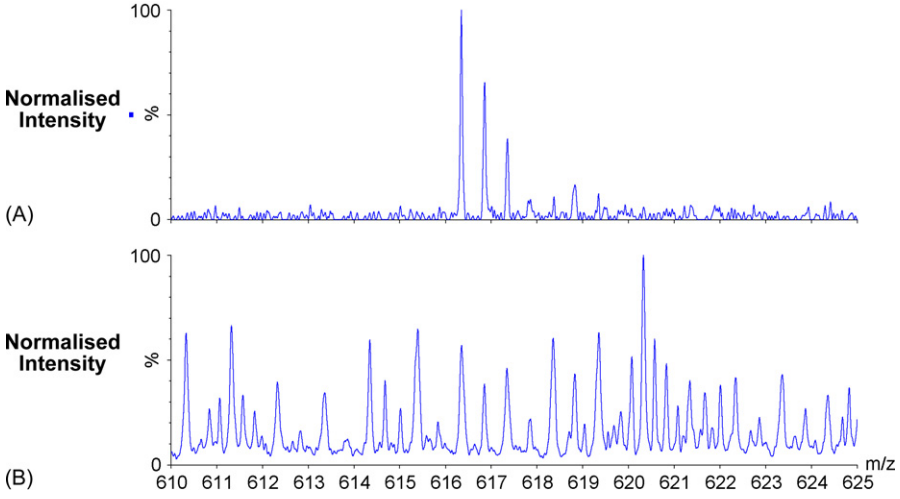

Fig. 17. (A) Reduced *m*/*z* range view of the data from Fig. 16(A); (B) reduced *m*/*z* range view of the data from Fig. 16(B).

arrangement of the lysozyme 7+ conformer, as can be seen in Fig. 14(B).

3.4. Protein digest study

The utility of ion mobility as an orthogonal separation technique to reduce mass spectral congestion is illustrated here through the separation of a mixture of four tryptically digested proteins. In Fig. 15, a plot of *m*/*z* versus arrival time for the electrosprayed ions can be seen following separation in the TWIMS. It is notable that the ions broadly fall into bands, which previous work has shown [40,41] is as a result of the different charge states of the peptides present. Charge state, *z*, is an important factor in determining the overall mobility of an ion species as is apparent from Eq. (1). The largest difference in mobility occurs between singly and the multiply charged species and is highlighted by the diagonal line in Fig. 15. As such this indicates that for ions of the same *m*/*z* value but different charge state, separation is possible. Alternatively, at a given arrival time, the singly charged species present will be of lower *m*/*z* value than the multiply charged species, as can be seen in Fig. 16(A) for the mobility slice from 4.9 to 5.2 ms. By comparison with the non-mobility-separated mass spectrum in Fig. 16(B) it can be seen that use of mobility separation has significantly reduced the mass spectral complexity, as is further illustrated in Fig. 17 where an expanded *m*/*z* view from 610 to 625 of these data is shown. This utility alone has significant potential in improving limits of detection for samples through effective background removal and is applicable to any complex mixture where the ions of interest have different mobility from the background ions.

4. Conclusion

In general the mobility separation characteristics of the TWIMS device have been shown to be similar to drift tube devices, which use a constant dc axial field to drive the separation, although the relationship between measured arrival times and mobility is different from the drift tubes. Previous work has

indicated that mobility calibration of the TWIMS is possible for large protein complexes using species of known collision cross-section [26]. This area requires further investigation for lower *m/z* species.

The utility of the instrument for investigating the conformational forms of multiply charged protein ions has been demonstrated, along with the capability to probe the energetics behind rearrangement of different conformers through use of collisional activation. Whilst the resolving power of the TWIMS is not as high as some drift tube systems, the separation capability is valuable for reducing mass spectral complexity, as has been shown for the a complex digest mixture where removal of singly charged background facilitates detection of lower level multiply charged peptide ions.

A particular advantage of the TWIMS device over most drift tubes is that through use of ion accumulation and radial ion confinement, the sensitivity of the mass spectrometer is not compromised when operating in mobility mode, allowing investigations on analytically significant levels of sample.

Overall, the data presented here illustrate that the incorporation of a high transmission travelling wave-based ion mobility separator within a quadrupole/oa-Tof geometry instrument shows significant promise for use in the characterisation of biological systems.

Acknowledgement

J.H. Scrivens, J.P. Williams and M.T. Bowers thank DEFRA for research funding.

References

[1] See articles in Nature (Insight) 426 (6968) (2003) 883–909.
[2] T. Wyttenbach, G.v. Helden, M.T. Bowers, J. Am. Chem. Soc. 118 (1996) 8355.
[3] D.E. Clemmer, R.R. Hudgins, M.F. Jarrold, J. Am. Chem. Soc 117 (1995) 10141.
[4] D.E. Clemmer, M.F. Jarrold, J. Mass Spectrom. 32 (1997) 577.
[5] T. Wyttenbach, M.T. Bowers, Top. Curr. Chem. 225 (2003) 207.
[6] J.A. McLean, B.T. Ruotolo, K.J. Gillig, D.H. Russell, Int. J. Mass Spectrom. 240 (2005) 301.
[7] P.E. Barran, N.C. Polfer, D.J. Campopiano, D.J. Clarke, P.R.R. Langridge-Smith, R.J. Langley, J.R.W. Govan, A. Maxwell, J.R. Dorin, R.P. Millar, M.T. Bowers, Int. J. Mass Spectrom. 240 (2005) 273.
[8] E.A. Mason, E.W. McDaniel, The Mobility and Diffusion of Ions in Gases, Wiley, New York, 1973.
[9] E.A. Mason, E.W. McDaniel, Transport Properties of Ions in Gases, Wiley, New York, 1988.
[10] J. Gidden, M.T. Bowers, J. Phys. Chem. B 107 (2003) 12829.
[11] M.D. Leavell, S.P. Gaucher, J.A. Leary, J.A. Taraszka, D.E. Clemmer, J. Am. Soc. Mass Spectrom. 13 (2002) 284.
[12] C.S. Hoaglund, S.J. Valentine, D.E. Clemmer, Anal. Chem. 69 (1997) 4156.
[13] S. Myung, Y.J. Lee, M.H. Moon, J. Taraszka, R. Sowell, S. Koeniger, A.E. Hilderbrand, S.J. Valentine, L. Cherbas, P. Cherbas, T.C. Kaufmann, D.F. Miller, Y. Mechref, M.V. Novotny, M.A. Ewing, C.R. Sporleder, D.E. Clemmer, Anal. Chem. 75 (2003) 5137.
[14] T. Wyttenbach, P.R. Kemper, M.T. Bowers, Int. J. Mass Spectrom. 212 (2001) 13.
[15] G. von Helden, T. Wyttenbach, M.T. Bowers, Int. J. Mass Spectrom. Ion Process. 146–147 (1995) 349.
[16] K.J. Gillig, B.T. Ruotolo, E.G. Stone, D.H. Russell, Int. J. Mass Spectrom. 239 (2004) 43.
[17] A.S. Woods, M. Ugarov, T. Egan, J. Koomen, K.J. Gillig, K. Fuhrer, M. Gonin, J.A. Schultz, Anal. Chem. 76 (2004) 2187.
[18] G. Javahery, B. Thomson, J. Am. Soc. Mass Spectrom. 8 (1997) 697.
[19] K. Thalassinos, S. Slade, K.R. Jennings, J.H. Scrivens, K. Giles, J. Wildgoose, J. Hoyes, R.H. Bateman, M.T. Bowers, Int. J. Mass Spectrom. 236 (2004) 55.
[20] Y. Guo, J. Wang, G. Javahery, B.A. Thomson, K.W.M. Siu, Anal. Chem. 77 (2005) 266.
[21] Y.J. Lee, C.S. Hoaglund-Hyzer, J.A. Leary, J.A. Taraszka, G.A. Zientara, A.E. Counterman, D.E. Clemmer, Anal. Chem. 73 (2001) 3549.
[22] K. Tang, A.A. Shvartsburg, H.N. Lee, D.C. Prior, M.A. Buschbach, F. Li, A.V. Tolmachev, G.A. Anderson, R.D. Smith, Anal. Chem. 77 (2005) 3330.
[23] S.I. Merenbloom, S.L. Koeniger, S.J. Valentine, M.D. Plasencia, D.E. Clemmer, Anal. Chem. 78 (2006) 2802.
[24] C.S. Hoaglund, S.J. Valentine, C.R. Sporleder, J.P. Reilly, D.E. Clemmer, Anal. Chem. 70 (1998) 2236.
[25] K. Giles, S.D. Pringle, K.R. Worthington, D. Little, J.L. Wildgoose, R.H. Bateman, Rapid Commun. Mass Spectrom. 18 (2004) 2401.
[26] B.T. Ruotolo, K. Giles, I. Campuzano, A.M. Sandercock, R.H. Bateman, C.V. Robinson, Science 310 (2005) 1658.
[27] D. Gerlich, In state-selected and state-to-state ion molecule reaction dynamics. Part 1. Experimental, in: C.Y. Ng, M. Baer (Eds.), Advances in Chemical Physics Series, vol. LXXXII, John Wiley & Sons, 1992.
[28] A. Gill, K.R. Jennings, T. Wyttenbach, M.T. Bowers, Int. J. Mass Spectrom. 195–196 (2000) 685.
[29] A.E. Counterman, S.J. Valentine, C.A. Srebalus, S.C. Henderson, C.S. Hoaglund, D.E. Clemmer, J. Am. Soc. Mass Spectrom. 9 (1998) 743.
[30] S.L. Bernstein, T. Wyttenbach, A. Baumketner, J.E. Shea, G. Bitan, D.B. Teplow, M.T. Bowers, J. Am. Chem. Soc. 127 (2005) 2075.
[31] C. Wu, W.F. Siems, J. Klasmeier, H.H. Hill Jr., Anal. Chem. 72 (2000) 391.
[32] A.M. Last, C.V. Robinson, Curr. Opin. Chem. Biol. 3 (1999) 564.
[33] A.J. Heck, R.H. Van Den Heuvel, Mass Spectrom. Rev. 23 (2004) 368.
[34] Z. Takats, J.M. Wiseman, B. Gologan, R.G. Cooks, Anal. Chem. 76 (2004) 4050.
[35] Z. Ouyang, Z. Takats, T.A. Blake, B. Gologan, A.J. Guymon, J.M. Wiseman, J.C. Oliver, V.J. Davisson, R.G. Cooks, Science 301 (2003) 1351.
[36] S.J. Valentine, J.G. Anderson, A.D. Ellington, D.E. Clemmer, J. Phys. Chem. B 101 (1997) 3891.
[37] R.A. Sowell, S.L. Koeniger, S.J. Valentine, M.H. Moon, D.E. Clemmer, J. Am. Soc. Mass Spectrom. 15 (2004) 1341.
[38] R.W. Purves, D.A. Barnett, B. Ells, R. Guevremont, J. Am. Soc. Mass Spectrom. 12 (2001) 894.
[39] S.L. Koeniger, S.I. Merenbloom, D.E. Clemmer, J. Phys. Chem. B 110 (2006) 7017.
[40] J.A. Taraszka, A.E. Counterman, D.E. Clemmer, Fresen. J. Anal. Chem. 369 (2001) 234.
[41] C.S. Hoaglund-Hyzer, Y.J. Lee, A.E. Counterman, D.E. Clemmer, Anal. Chem. 74 (2002) 992.